Protoplasma 125, 13—23 (1985)

PROTOPLASMA

The Ultrastructure of the Plasmodesmata of the Salt Glands of *Tamarix* as Revealed by Transmission and Freeze-Fracture Electron Microscopy

W. W. THOMSON * and KATHRYN PLATT-ALOIA

Department of Botany and Plant Sciences, University of California, Riverside, California

Received February 8, 1984
Accepted July 11, 1984

Summary

Numerous plasmodesmata occur in the walls between the secretory cells of *Tamarix* salt glands. The plasmalemma bounds the plasmodesmata and is continuous from cell to cell. In freeze-fracture, the e-face of the plasmalemma within the plasmodesmata is virtually devoid of intramembranous particles while, in contrast, the p-face is decidedly enriched with particles. The axial components appear to be a tightly curved membrane bilayer, as judged from measurements and their appearance in freeze-fracture, and the e-face of this membrane is also devoid of particles. Observations from both thin sections and freeze-fracture replicas indicate the presence of a circular cluster of six particles around the axial component near the cytoplasmic termini of the plasmodesmata. These particles extend from the p-face of the axial component to the p-face of the plasmalemma. These observations are summarized in a model.

Keywords: Plasmodesmata; Ultrastructure; Freeze-fracture; Salt glands.

1. Introduction

Although most evidence is indirect and correlative, plasmodesmata are considered to have a direct role in the movement of substances and/or the channeling of biophysical and biochemical signals from cell to cell in plant tissues (JUNIPER and BARLOW 1969, TUCKER 1982, GUNNING and ROBARDS 1976 and papers therein). However, as GUNNING and OVERALL (1983) have pointed out, hypotheses as to the mechanisms of plasmodesmatal function have been derived primarily from ultrastructural observations. To date, almost all ultrastructural studies on plasmodesmata have involved thin-section, transmission electron microscopy, and two primary limitations overshadow interpretations and models derived from these studies: a) the everpresent lack of basic information on the nature of density patterns in electron micrographs in regard to the chemical constituents of the biological material, and b) plasmodesmata are often smaller than the thickness of a thin section, and fine details of their structure are therefore frequently masked and obscured (GUNNING and OVERALL 1983).

With these inherent restrictions imposed on studies of thin sections and the virtual absences of information from freeze-fracture investigations (WILLISON 1976, GUNNING and OVERALL 1983), our understanding of the macromolecular organization of these important structures is seriously limited. It is not clear why plasmodesmata have not been previously amenable to freeze-fracture examination. However, in our continuing studies on plant salt glands, we have found that freeze-fracture images of the plasmodesmata of the gland cells are readily obtained. Thus, the essence of this report is the nature of the macromolecular organization of these plasmodesmata as revealed by freeze-fracture and as correlated with images from thin sections.

2. Methods

For transmission electron microscopy, small terminal portions of sprigs of *Tamarix aphylla* L. were fixed for 1 to 2 hours in 2.5% glutaraldehyde in 0.1 M potassium phosphate buffer, pH 7.0. A part of this material was subsequently post-fixed in 1% osmium tetroxide with the same buffer and then processed by standard dehydration and embedment in epoxy plastic (SPURR 1969). Attempts to enhance

* Correspondence and Reprints: Department of Botany and Plant Sciences, University of California, Riverside, CA 92521, U.S.A.

staining with tannic acid and $FeCl_3$ (OLESON 1979, OVERALL *et al.* 1982) were unsuccessful, possibly because this tissue has a high content of endogenous tannins. However, decided enhancement of image quality was achieved by staining the thin sections on the grids with hot, saturated alcoholic uranyl acetate for 20 to 30 minutes (LOCKE and KRISHNAN 1971) followed by a normal staining with lead citrate (REYNOLDS 1963).

Rotational image reinforcements were done following strictly the procedures and precautions of HORNE and MARKHAM (1972). When the dark field mode of the microscope was used, the beam tilt angle was $+ 13 \times 10^{-3}$ rad.

For freeze-fracture electron microscopy, a portion of the above material was taken after the primary fixation with glutaraldehyde. This material was rinsed 15 to 30 minutes in the same buffer and infiltrated stepwise (5, 10, 15, and 20%; 30 minutes each step) with glycerol made in 0.1 M potassium phosphate buffer. The tissue was kept in 20% glycerol solution overnight. The tissue was then mounted in gold-nickel planchettes and quickly frozen in liquid propane cooled by liquid nitrogen. Fracturing and replication was with a Balzers 301 freeze-fracture device equipped with a quartz thin-film monitor and electron beam guns for both platinum and carbon. The vacuum was $< 2 \times 10^{-6}$ torr, and the temperature of the sample was -115 °C. Replicas were cleaned by a sequential treatment with: a) alcoholic KOH (95% EtOH, 12% KOH); b) 70% sulfuric acid; and c) chromic acid (PLATT-ALOIA and THOMSON 1983). The replicas were picked up on formvar-coated freeze-fracture grids. The nomenclature used to identify the fracture faces was that of BRANTON *et al.* (1975).

All material was studied and photographed with a Philips EM 400.

3. Observations

The salt glands consist of six secretory cells (Figs. 1 and 2), and as reported previously (THOMSON and LIU 1967), all the gland cells are interconnected via plasmodesmata (Fig. 1). The walls between the secretory cells are quite thin, measuring about 40 nm in width, and characteristically, in all the glands we have examined, an electron transparent gap occurs between the wall and the adjacent plasmalemma (Fig. 3 *g*). This gap may be artefactual (BROWNING and GUNNING 1977), although no such gap was present along the innermost wall of the basal cell or the walls of the underlying mesophyll cells (not shown). Longitudinal sections indicate that the smallest diameter of the plasmodesmata of the secretory cells occurs where they traverse the walls (Figs. 3, 5, and 6), and measurements indicate that in this region they are approximately 55 nm in diameter—*i.e.*, measuring from the outer margin of the plasmalemma on both sides of the plasmodesmata. Similarly and consistently, the smallest diameter of plasmodesmata in cross-section measured approximately 55 nm (Fig. 7). The plasmalemma borders the plasmodesmata (Figs. 5 and 6) and is continuous from cell to cell, but no neck constriction was found. As reported for other material (see GUNNING and ROBARDS 1976 and articles therein), in cross sections, a somewhat clear sleeve or collar, about 4 nm in width, occurred between the plasmalemma and the surrounding fibrous wall (Fig. 7 *c*), and in favorable longitudinal sections, the sleeve appeared as a thin, lightly fibrous region of the wall (Figs. 5 and 6). The nature of this sleeve as well as the continuity of the plasmalemma through the plasmodesmata were more readily apparent in the dark field micrographs than in normal bright-field transmission images (compare Fig. 5 to Fig. 6).

In both longitudinal and cross sections, an axial component in the center of the plasmodesmata was observed (Figs. 5–7). In cross sections, it measured approximately 22 nm in diameter. In oblique sections of the walls the plasmodesmata are often cut in cross section at different planes relative to the surface of the cell (ROBARDS 1976). In transverse sections close to the cytoplasm, we observed a further substructure in that six translucent subunits occurred around the axial component, positioned between the axial component and the bounding plasmalemma of the plasmodesmata (Fig. 7). These subunits were delimited by thin, dense radial spokes that also extended from the axial component to the plasmalemma (Fig. 7). Rotary image reinforcement analysis of these cross sections further indicated a radial symmetry of six subunits with a center-to-center spacing of 14 nm (Fig. 8). Continuities of the endoplasmic reticulum with the axial component were observed (Fig. 3).

3.1. Freeze Fracture

In freeze-fracture replicas, the p-face, or protoplasmic face, of the plasmalemma of the secretory cells was readily recognized and characterized by a decided enrichment of intramembranous particles (Fig. 9). Contrariwise, but equally consistent, the e-face, or exoplasmic face, was recognized and identified by having many fewer intramembranous particles (Fig. 9). Longitudinal fractures of the plasmodesmata revealed that this general pattern also existed for the plasmalemma in the plasmodesmata, *i.e.*, the outer, e-face of the plasmalemma of the plasmodesmata had very few intramembranous particles (Figs. 10–12), while the p-face was enriched in intramembranous particles (Figs. 13–15); however, no particular packing order or pattern of organization of the particles, one to another, was observed.

Occasionally, exceedingly large fracture planes of both the e- and p-faces of the plasmalemma of the secretory cells were found. (For example, in Fig. 16 the p-face of almost the entire plasmalemma bordering a periclinal

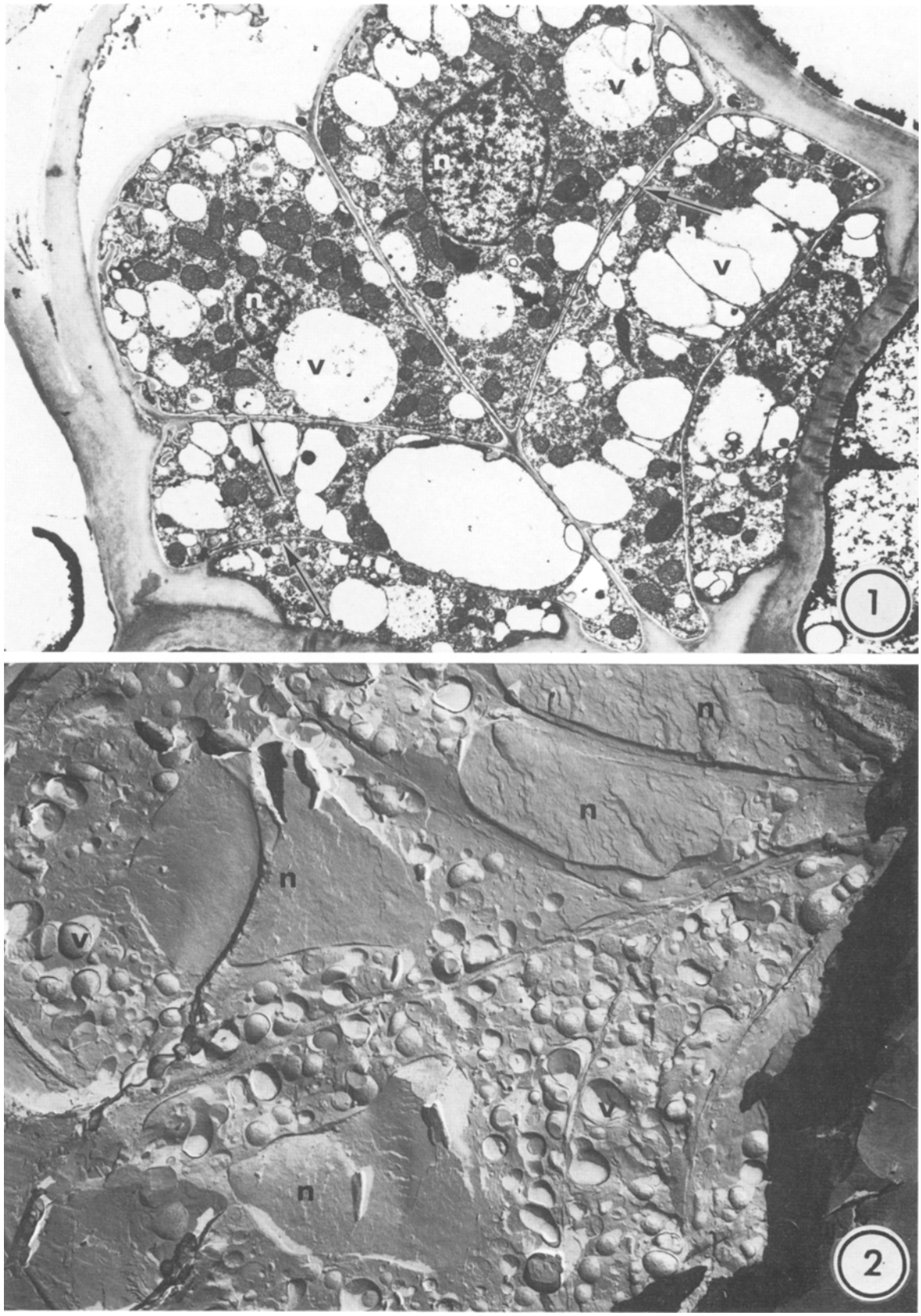

Fig. 1. A near median thin section of a salt gland illustrating that it is composed of six secretory cells. The arrows indicate the plasmodesmata in the walls of the secretory cells that are the subject of this article. × 6,800. *n* nuclei, *v* vacuoles

Fig. 2. A corresponding, near median, freeze-fracture replica of a gland similar to that in Fig. 1. Again, major portions of all six secretory cells are observed. × 6,800. *n* nuclei, *v* vacuoles

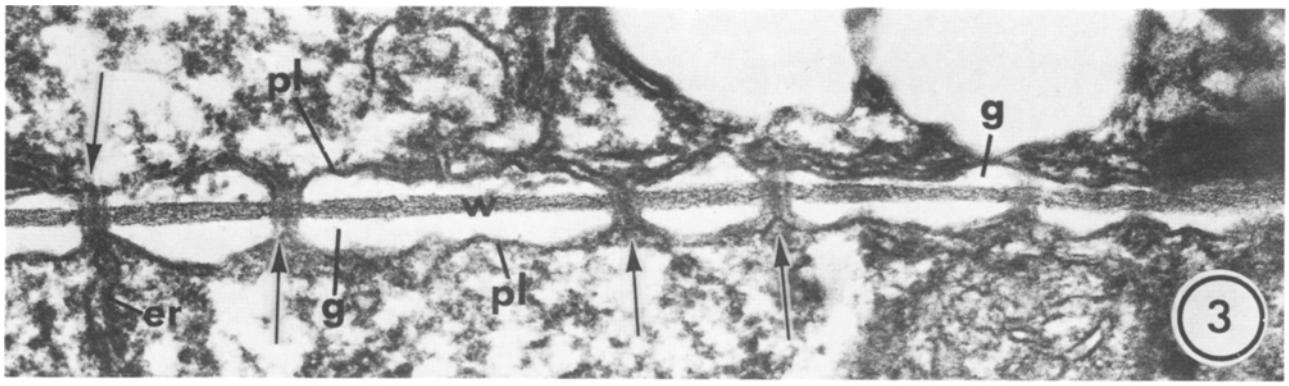

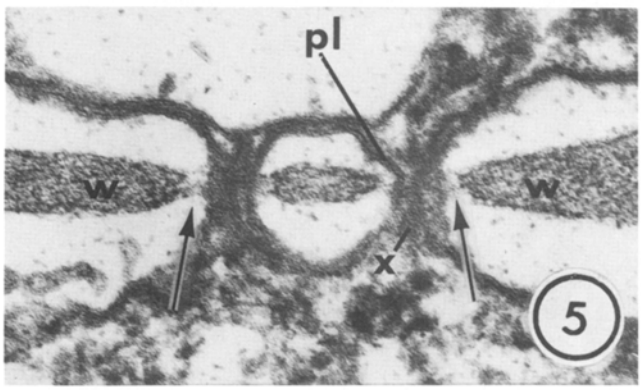

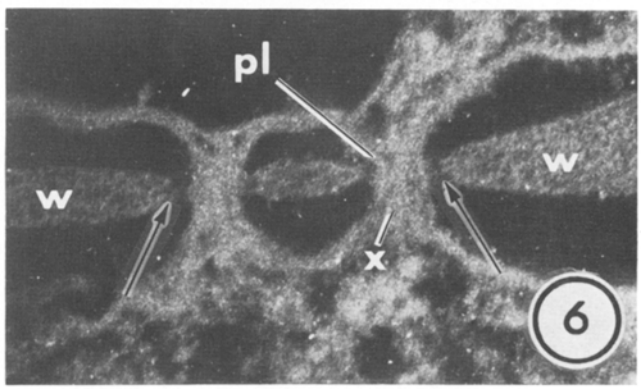

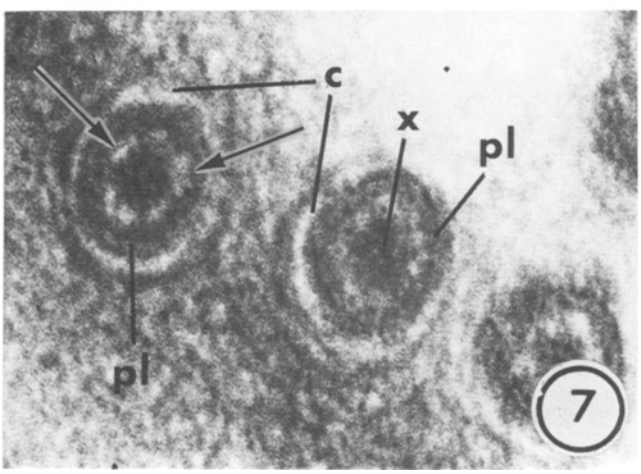

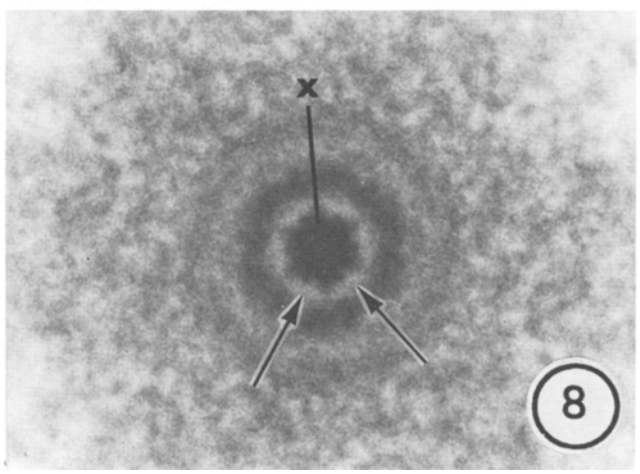

Figs. 3–8

wall of a secretory cell is present in the replica.) These replicas were pimpled with raised, cone-like p-face fractures of the plasmodesmata (Figs. 16 and 18). From such replicas, it was determined that there were approximately 24 plasmodesmata per μm^2 of the cell surface and that at least 1,495 plasmodesmata existed in the periclinal walls between two secretory cells. Plasmodesmata also exist in the central anticlinal walls of the glands, and although counts were not made, direct observation indicates the number was much less than in the periclinal walls.

In replicas where the p- and e-faces of the plasmalemma were revealed clearly, it was obvious that the fracture often extended along the complete length of the plasmodesmata and on into the plasmalemma of the adjacent cells (Figs. 10–15). However, in many replicas it was also obvious that the fracture extended for various distances into the plasmodesmata before coursing across the plasmodesmata and following back out along a fracture face of the plasmalemma (Figs. 17 and 18). Frequently, in such e-face cross fractures of plasmodesmata, a circular cluster of six particles was observed surrounding a central core element (Fig. 17). The central core element we have interpreted as a fracture of the axial component, and the surrounding particles appeared to extend from the axial component to the e-face of the plasmalemma (Fig. 17). The axial component measured approximately 12 nm in diameter. The surrrounding particles measured about 10 nm with a center-to-center spacing of 14 nm. High magnification of corresponding p-face fractures of the plasmodesmata revealed a complimentary pattern to that observed with e-face cross fractures (Fig. 18). Estimating from the angle of shadowing and shadow length, these cross fractures occurred at different relative positions within the plasmodesmata (Fig. 18). Where the cross fracture was relatively shallow, the plasmodesmata resembled a volcanic cinder-cone in which the surface of the cone could be identified as a continuum of the particle-enriched p-face of the plasmalemma (Fig. 18, arrow). In these cross fractures, the center of the cone appeared as a featureless depression. In cross fractures that occurred somewhat deeper in the plasmodesmata, the center position of the cone was occupied with a central element, approximately 16 nm in diameter, that was surrounded by a cluster of six particles (Fig. 18, arrowheads). These particles measured approximately 13 nm in diameter and had a center-to-center spacing of 16 nm.

Occasionally, p-face cross fractures occurred more deeply within the plasmodesmata, and short, "rod-like" projections extended from the center of conical-shaped fractures of the plasmodesmata (Fig. 19). These "rod-like" projections measured about 13 nm in diameter.

As will be discussed later, we consider the axial component to consist of a tightly curved, cylindrical bilayer as suggested by OVERALL *et al.* (1982) and GUNNING and OVERALL (1983), and thus we interpret the "rod-like" projection to be an e-face extension of the inner half of this membrane. Of note is the absence of intramembranous particles in this membrane face (Fig. 19). Unfortunately, we were unable to find the complementary p-face replicas of the axial component.

4. Discussion

A summary of our observations on the plasmodesmata of the secretory cells of these salt glands is presented in the model in Fig. 20. There are several salient features to be noted. First, the e-face of the plasmalemma within the plasmodesmata was virtually devoid of intramem-

Fig. 3. A portion of a wall between two secretory cells containing several plasmodesmata (arrows). An electron-translucent gap (*g*) exists between the plasmalemma (*pl*) and the wall (*w*). Continuity of the endoplasmic reticulum (*er*) with the axial component of the plasmodesmata is evident. × 72,000

Fig. 4. A portion of a wall (*w*) between two secretory cells in which freeze-fracture images of plasmodesmata are clearly evident (arrows). × 72,000

Fig. 5. A longitudinal section of two plasmodesmata in a wall (*w*) between two secretory cells. The plasmalemma (*pl*) is continuous through the plasmodesmata, and the axial component (*x*) is evident as a solid central component. The collar in the wall around the plasmodesmata is evident as an extreme thinning of the wall in this region (arrows). × 120,000

Fig. 6. This is a dark-field image of the same plasmodesmata illustrated in Fig. 5. The dark-field image emphasizes many of the features described in Fig. 5. × 120,000

Fig. 7. A transverse section of three plasmodesmata. The electron-translucent collar (*c*) between the wall and the plasmalemma (*pl*) is quite obvious, as is the solid, electron-dense nature of the axial component (*x*). Six electron-transparent subunits (arrows) apparently occur between the axial component and the plasmalemma. × 390,000

Fig. 8. A rotational image reinforcement of the plasmodesma on the left side of Fig. 7. A circular pattern of six electron-translucent subunits exist between the axial component (*x*) and the outer dense band at the plasmalemma. × 450,000

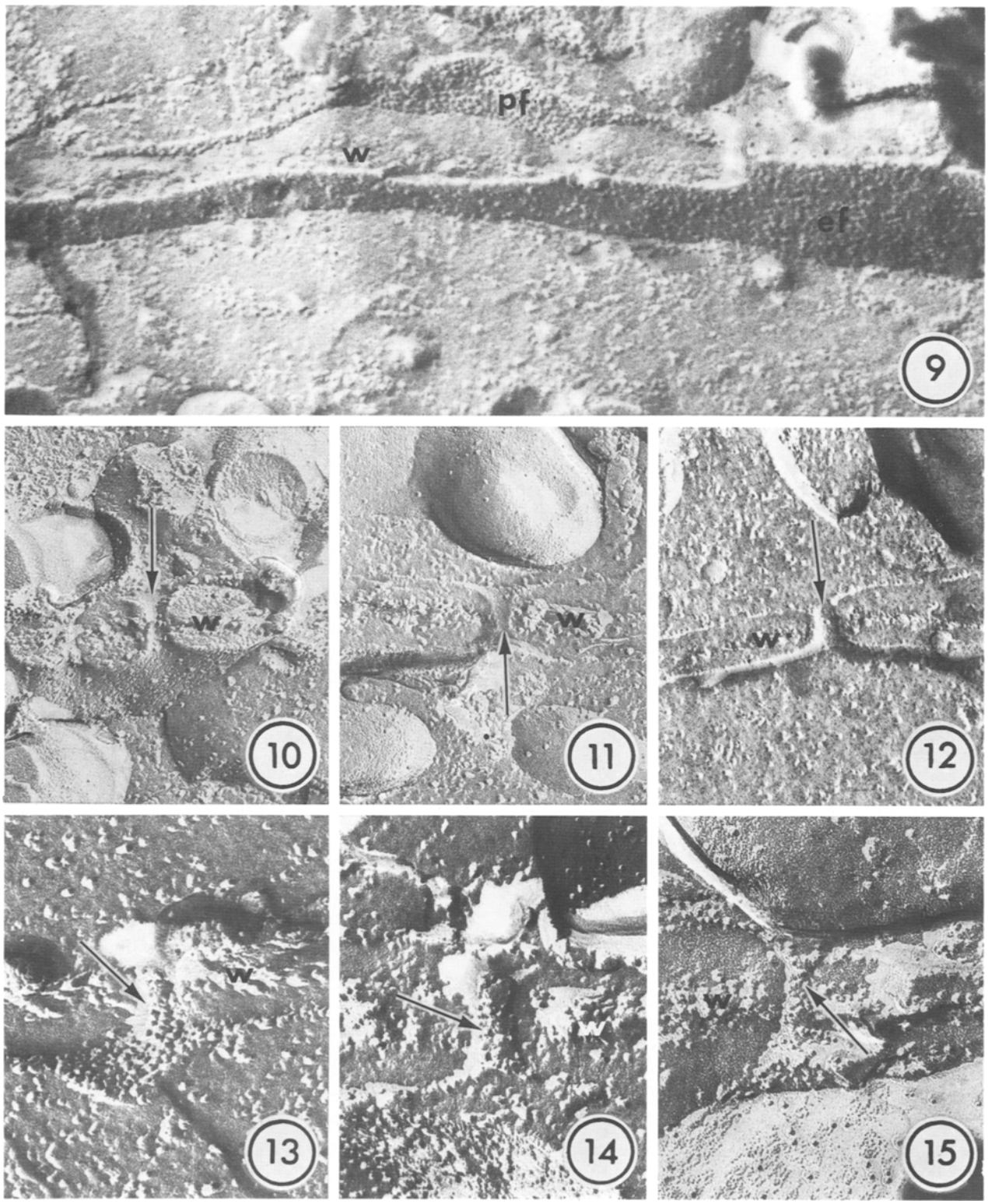

Fig. 9. A freeze-fracture image of the wall (*w*) between two secretory cells. The p-face (*pf*) of the bounding plasmalemma is enriched in intramembranous particles while the e-face (*ef*) has many fewer. × 91,000

Figs. 10–12. These figures (arrows) illustrate the e-face of the plasmalemma within the plasmodesmata and the lack of intramembranous particles in this face of the membrane. × 142,000

Figs. 13–15. These figures (arrows) illustrate the p-face of the plasmalemma within the plasmodesmata and the enrichment of intramembranous particles in this face of the membrane. × 142,000

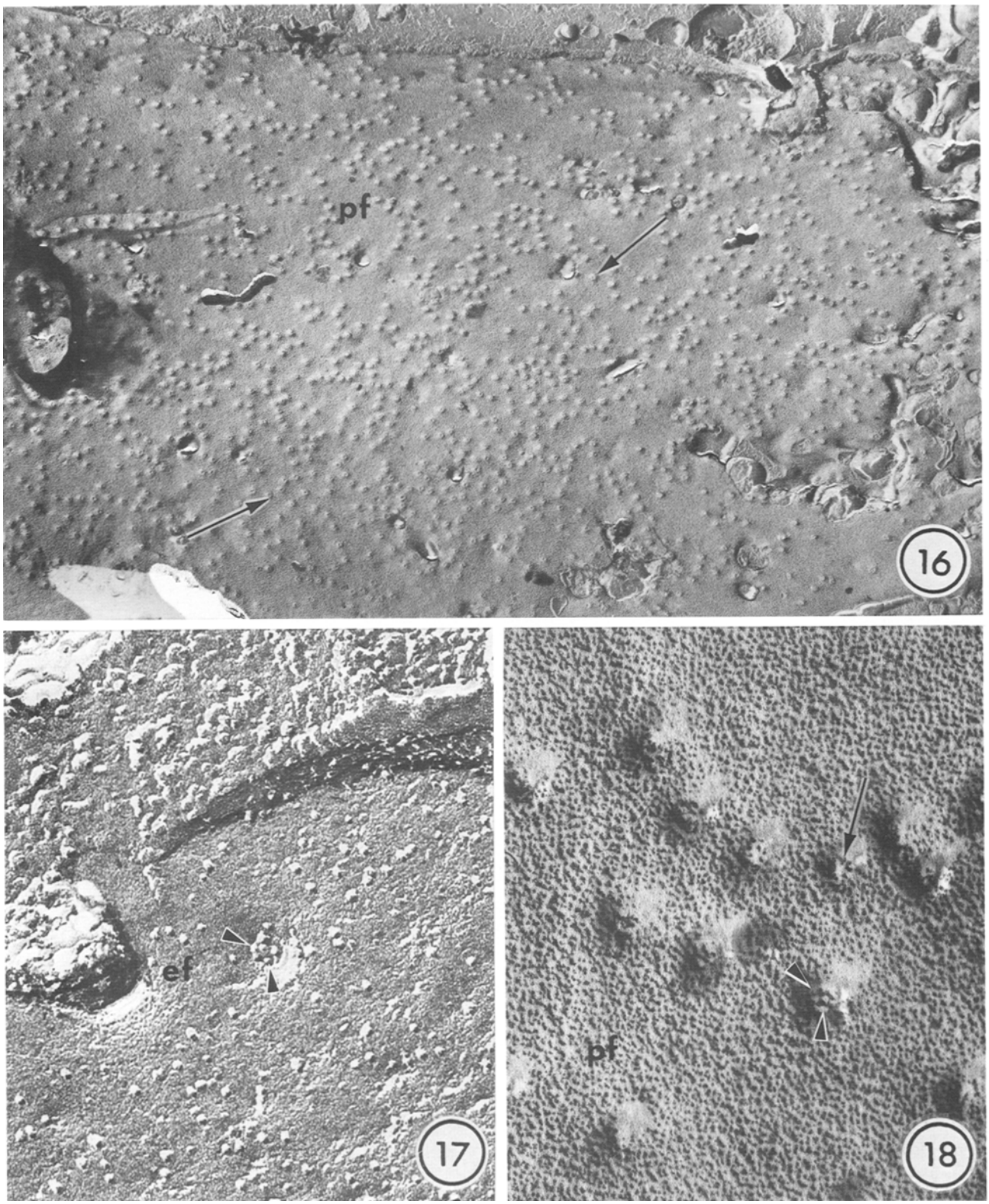

Fig. 16. A portion of a large p-face (*pf*) fracture of the plasmalemma bounding a secretory cell. The fracture images of the numerous plasmodesmata appear as raised pimples (arrows). × 14,000

Fig. 17. An enlarged example of an e-face (*ef*) cross fracture of a plasmodesma indicating the presence of five, possibly six, subunits (arrowheads) surrounding a central core unit. × 145,000

Fig. 18. An enlarged example of a p-face (*pf*) cross fracture of plasmodesmata. A shallow cross fracture is indicated by the arrow; however, a deeper cross fracture illustrates the presence of six subunits (arrowheads) surrounding a central core unit. × 93,000

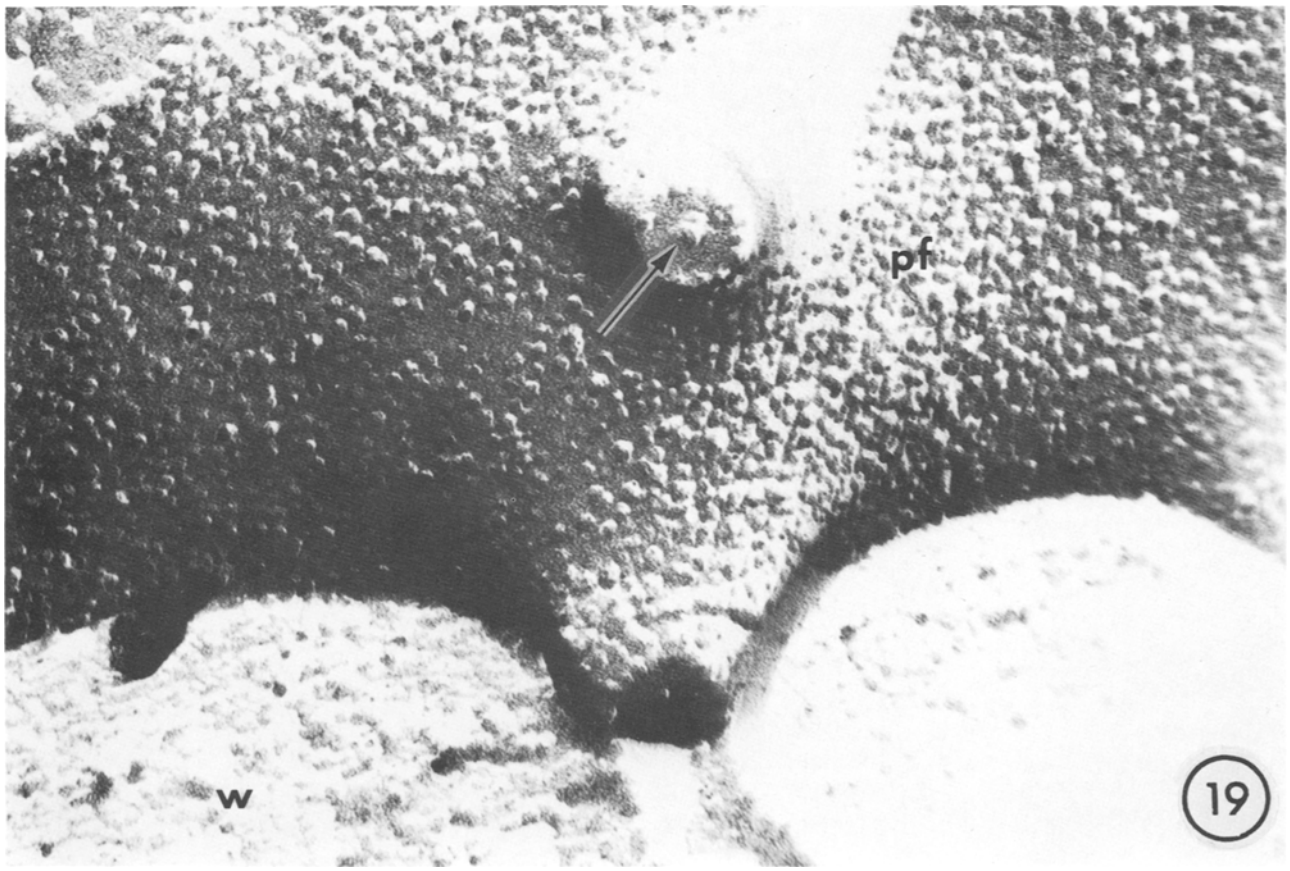

Fig. 19. A high magnification view of a p-face (*pf*) cross fracture of two plasmodesmata. The enrichment of intramembranous particles in this fracture plane of the plasmalemma is quite obvious, and the arrow indicates an e-fracture face of the central, axial element. × 225,000. *w* wall

branous particles while in contrast, the p-face was enriched in such particles. The plasmalemma of the secretory cells also had an asymmetric distribution of intramembranous particles with the p-face far more enriched than the e-face. The nature of intramembranous particles in the plasmalemma of plant cells is not now known, and it is probably premature to speculate as to their possible role(s) in the p-face within the plasmodesmata. However, as it is now common in freeze-fracture microscopy, we assumed these particles to be integral membrane proteins. As far as the smooth nature of the e-face, it may well indicate that the lipid of this half of the membrane might be in a gel, or nonfluid state, since it is known that phase separation of particular lipids into fluid and gel domains can occur. Integral membrane proteins have been shown to prefer the more fluid regions (GRANT 1983), thus resulting in particle-free areas corresponding to gel phase lipid in freeze-fracture images (JAMES and BRANTON 1973). The absence of e-face particles in the plasmalemma within the plasmodesmata does imply a particular differentiation between this region and that of the contiguous plasmalemma bounding the cell where particles are prevalent. This consideration was also suggested by OVERALL *et al.* (1982).

The nature of the axial component is portrayed as a tightly curved lipid bilayer. This is in agreement with OVERALL *et al.* (1982) and GUNNING and OVERALL (1983) who have suggested that the axial component was a cylindrical extension of the endoplasmic reticulum in which the lumen of the endoplasmic reticulum was virtually eliminated by the tight curvature and packing of the e-face lipids of this membrane system. We support this view for the following reasons: in thin sections, the axial component measured about 22 nm. This diameter is approximately twice that reported by OVERALL *et al.* (1982) with roots of *Azolla*. However, a bilayer 22 nm in diameter would be tightly curved in nature, and parenthetically, the diameter of plasmodesmata and the axial component has been reported to vary in dimensions in different tissues (ROBARDS 1976). Also, in freeze-fracture, the axial element measured 12 nm in e-face fractures, 16 nm in p-face fractures, and the rod-like projection of the axial

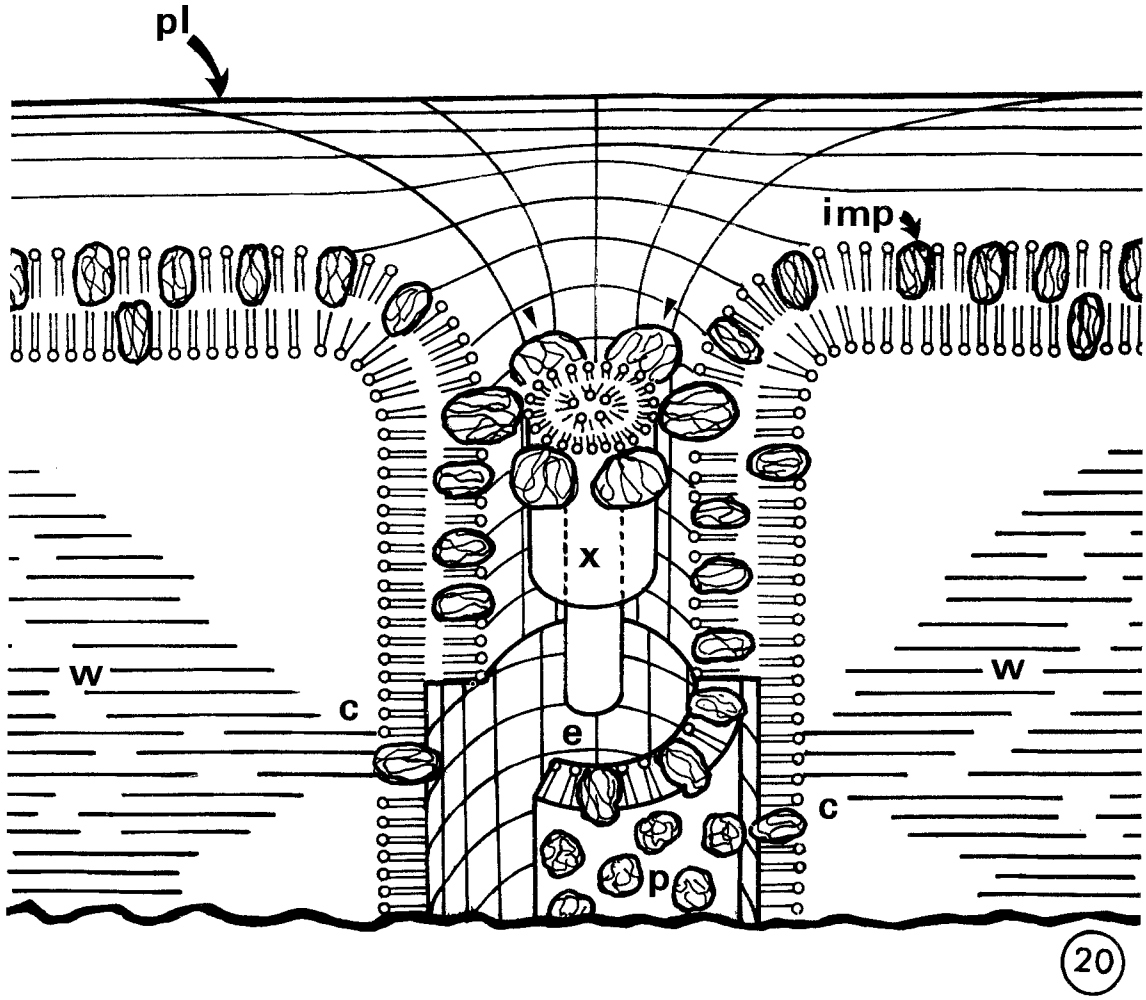

Fig. 20. This model depicts the organization of the plasmodesmata of the salt glands as revealed in the thin section and freeze-fracture, electron microscope studies reported herein. The various components identified are: *pl* plasmalemma, *w* wall, *c* collar, *p* p-face, *e* e-face, *imp* integral membrane protein, *x* bilayered, axial component, arrowheads = six radially arranged, presumably proteinaceous subunits

component measured approximately 13 nm in diameter. We consider these measurements to be consistent to each other considering the limitations imposed by the procedures used in preparation. Thus, we interpreted this projection to be an e-face cylinder of the inner lipid layer of the axial component. A diameter of 13–16 nm is consistent with what would be predicted by the OVERALL *et al.* (1982) model. The smooth surface of the wall of this projection, as observed in freeze-fracture, suggests that it is an intramembrane face of a membrane lipid layer, assuming that in freeze-fracture the split occurred along the center of a membrane bilayer between the terminal, methyl groups of the adjacent fatty acids of the membrane lipids (PINTO DA SILVA and BRANTON 1970).

The absence of particles in the e-face is indicative that proteins are excluded from this layer of membrane within the plasmodesmata, a possibility also suggested by OVERALL *et al.* (1982). Unfortunately, the p-face of this membrane was not observed, and we have simply portrayed it as a lipid layer until more information can be obtained. Since we observed continuities of the endoplasmic reticulum with the axial component, we consider that the axial component is derived from the endoplasmic reticulum. Our observations are consistent with those in the literature where the continuity of the endoplasmic reticulum with the axial component has been clearly shown (LÓPEZ-SÁEZ *et al.* 1966, THOMSON 1969, FISHER and EVERT 1982, OVERALL *et al.* 1982) and evidence that elements of the endoplasmic reticulum are enclosed within plasmodesmata during the development of the cell plate and wall formation with cell division (HEPLER 1982). However, in the model presented, we have not pictured the continuity of the ER with the axial component.

In recent years, attention has been drawn to the tight

association of the plasmalemma with the axial component at the terminal neck(s) of the plasmodesmata (ROBARDS 1968 a, b, EVERT *et al.* 1977, OLESON 1979). In some tissues, the plasmodesmata are constricted at these places (ROBARDS 1976, OLESON 1979, OVERALL *et al.* 1982), and the possibility that these regions may have valve-like functions such as "sphincters" has been suggested (WILLISON 1976, OLESON 1979, OVERALL *et al.* 1982). Previously, ROBARDS (1968 b), using rotary image reinforcements of cross sections of plasmodesmata, reported that 11 subunits in a ring symmetry may exist as an annulus between the axial component and the plasmalemma. However, ZEE (1969) reported 14 radially arranged subunits, and more recently OLESEN (1979), nine. OVERALL *et al.* (1982) also suggested the possibility of nine subunits from studies of thin sections, but this was not claimed for certainty. Our studies on the plasmodesmata, using thin sections and optical rotary reinforcement, and particularly the observations from both p-face and e-face images from freeze-fracture, indicate the presence of six subunits arranged in a ring in this region and is portrayed as such. However, the variation in number of these subunits that has been reported for other tissues may be one of the important structural and functional differences between different types of plasmodesmata. The salt glands are highly specialized structures, and it might be expected that their plasmodesmata, although generally similar to other plasmodesmata, may differ in some particulars.

It could be assumed that changes in the macromolecular organization of the plasmodesmata would be indicative of different functional states. For example, WILLISON (1976) noted a variation in the distribution of e-face plasmalemma particles near the orifice of plasmodesmata which he suggested may be related to different functional conditions. We did not observe such variations with any aspect of the ultrastructural organization of these plasmodesmata. However, we have only been able to obtain replicas of the salt glands after fixation with glutaraldehyde and treatment with the cryoprotectant, glycerol. Both glutaraldehyde and glycerol have been reported to affect the distribution of intramembranous particles in some membrane systems (RASH and HUDSON 1979), and whether such effects have occurred with the salt glands is not known. Our conclusions are based on the observations we have. Hopefully, the application of different methods, such as extremely fast freezing rates, can be applied to the glands in the future. Such techniques might reveal variations, for example, in the "sphincter" complex, the axial component, and the plasmalemma of the plasmodesmata that will bear directly on functional considerations.

Finally, in this paper we have avoided the use of the term desmo-tubule (ROBARDS 1968 a) and have opted to identify the rod-like structure as the axial component of the plasmodesmata as suggested by LÓPEZ-SÁEZ *et al.* (1966). We prefer this designation for two reasons: first, our observations on the plasmodesmata of the secretory cells of the glands are consistent with those of OVERALL *et al.* (1982) with the roots of *Azolla* in that the axial component is not a tube but probably represents a tightly curved membrane bilayer with no internal lumen; and second, to identify the axial component as a tube without clear structural evidence has an unfortunate connotation in a functional sense.

Acknowledgements

We thank TOM DALLMAN for help with drawing the model. This investigation was supported in part by NSF grants PCM 80-03779 and PCM 83-02145.

References

BRANTON, D., BULLIVANT, S., GILULA, N. B., KARNOVSKY, M. J., MOOR, H., MUHLETHALER, K., NORTHCOTE, D. H., PACKER, L., SATIR, B., SATIR, P., SPETH, V., STAEHELIN, L. A., STEERE, R. L., WEINSTEIN, R. S., 1975: Freeze-etching nomenclature. Science (N.Y.) **190**, 54—46.

BROWNING, A. J., GUNNING, B. E. S., 1977: An ultrastructural and cytochemical study of the wall-membrane apparatus of transfer cells using freeze-substitution. Protoplasma **93**, 7—26.

EVERT, R. F., ESCHRICH, W., HEYSER, W., 1977: Distribution and structure of plasmodesmata in mesophyll and bundle-sheath cells of *Zea mays* L. Planta **136**, 77—89.

FISHER, D. G., EVERT, R. F., 1982: Studies of the leaf of *Amaranthus retroflexus* (*Amaranthaceae*): ultrastructure, plasmodesmatal frequency, and solute concentration in relation to phloem loading. Planta **155**, 377—387.

GUNNING, B. E. S., OVERALL, R. L., 1983: Plasmodesmata and cell-to-cell transport in plants. Bioscience **33**, 260—265.

— ROBARDS, A. W., 1976: Intercellular communication in plants: Studies on plasmodesmata, 387 pp. Berlin-Heidelberg-New York: Springer.

GRANT, C. W. M., 1983: Lateral phase separations and the cell membrane. In: Membrane fluidity in biology, Vol. 2 (ALOIA, R. C., ed.), pp. 131—150. New York: Academic Press.

HEPLER, P. K., 1982: Endoplasmic reticulum in the formation of the cell plate and plasmodesmata. Protoplasma **111**, 121—133.

HORNE, R. W., MARKHAM, R., 1972: Application of optical diffraction and image reconstruction techniques to electron micrographs. In: Practical methods in electron microscopy, Vol. 1, Part 2 (GLAUERT, A. M., ed.), pp. 327—434. Amsterdam: North Holland.

JAMES, R., BRANTON, D., 1973: Lipid- and temperature-dependent structural changes in *Acholeplasma laidlawii* cell membranes. Biochim. biophys. Acta **323**, 378—390.

JUNIPER, B. E., BARLOW, P. W., 1969: The distribution of plasmodesmata in the root tip of maize. Planta **89**, 352—360.

LOCKE, M., KRISHNAN, N., 1971: Hot alcoholic phosphotungstic acid and uranyl acetate as routine stains for thick and thin sections. J. Cell Biol. **50**, 550—556.

LÓPEZ-SÁEZ, J. F., GIMÉNEZ-MARTÍN, G., RISUEÑO, M. C. J., 1966: Fine structure of the plasmodesm. Protoplasma **61**, 81—84.

OLESON, P., 1979: The neck constriction in plasmodesmata: evidence for a peripheral sphincter-like structure revealed by fixation with tannic acid. Planta **144**, 349—358.

OVERALL, R. L., WOLFE, J., GUNNING, B. E. S., 1982: Intercellular communication in *Azolla* roots. I. Ultrastructure of plasmodesmata. Protoplasma **111**, 134—150.

PINTO DA SILVA, P., BRANTON, D., 1970: Membrane splitting in freeze-fracture etching. Covalently bound ferritin as a membrane marker. J. Cell Biol. **45**, 598—605.

PLATT-ALOIA, K. A., THOMSON, W. W., 1982: Freeze-fracture of intact plant tissues. Stain Technol. **57**, 327—334.

RASH, J. E., HUDSON, C. S., 1979: Freeze fracture: Methods, artifacts, and interpretations, 204 pp. New York: Raven Press.

REYNOLDS, E. S., 1963: The use of lead citrate at high pH as an electron-opaque stain in electron microscopy. J. Cell Biol. **17**, 208—212.

ROBARDS, A. W., 1968 a: Desmotubule—a plasmodesmatal substructure. Nature **218**, 784.

— 1968 b: A new interpretation of plasmodesmatal ultrastructure. Planta **82**, 200—210.

— 1976: Plasmodesmata in higher plants. In: Intercellular communication in plants: Studies on plasmodesmata (GUNNING, B. E. S., ROBARDS, A. W., eds.), pp. 15—53. Berlin-Heidelberg-New York: Springer.

SPURR, A. R., 1969: A low-viscosity epoxy resin embedding medium for electron microscopy. J. Ultrastruct. Res. **26**, 31—43.

THOMSON, W. W., 1969: Ultrastructural studies on the epicarp of ripening oranges. Proc. First Intern. Citrus Symp. Vol. **3**, 1163—1169.

— LIU, L. L., 1967: Ultrastructural features of the salt gland of *Tamarix aphylla* L. Planta **73**, 201—220.

TUCKER, E. B., 1982: Translocation in the staminal hairs of *Setcreasea purpurea*. I. A study of cell ultrastructure and cell-to-cell passage of molecular probes. Protoplasma **113**, 193—201.

WILLISON, J. H. M., 1976: Plasmodesmata: a freeze-fracture view. Can. J. Bot. **54**, 2842—2847.

ZEE, S.-Y., 1969: The fine structure of differentiating sieve elements of *Vicia faba*. Aust. J. Bot. **17**, 441—456.